CMOS-ESPI-system with in-line digital phase stabilization using unresolved speckles

Heinz Helmers[1], Daniel Carl, Thorsten Sievers
Carl-von-Ossietzky University Oldenburg, Department of Physics

ABSTRACT

In combination with phase shifting techniques electronic speckle pattern interferometry (ESPI) is a versatile tool in the field of deformation measurements. However, in applications outside the laboratory, it suffers from the influence of external disturbances, especially mechanical vibrations and temperature fluctuations. These effects result in global phase fluctuations that are constant over the field of measurement, but vary in time. Phase fluctuations of this kind can be compensated by an active phase stabilization system.

In previous papers we introduced a DSP-controlled digital phase stabilization system on the basis of a synthetic heterodyne technique which needs no additional optical components in the ESPI set-up and stabilizes the phase at one point of the field of measurement. In this paper we will report on further improvements of the system. The functionality of further components has been integrated in the DSP, making the handling of the system and the variation of parameters of the control system even simpler. Furthermore, a high speed CMOS-camera with high full well capacity is used in the set-up instead of a CCD-camera and the system is operated with unresolved speckles. This CMOS-camera makes not only the tracking of fast deformation processes and the observation of objects with strongly varying brightness possible, but it can simultaneously generate the input signal for the control system. Finally, the control signal can be analyzed in order to get further information about object movements, especially rigid body motions and the sign of an object deformation itself.

Keywords: Electronic speckle pattern interferometry (ESPI), unresolved speckles, phase stabilization, CMOS-sensors

1. INTRODUCTION

In an electronic speckle pattern interferometer (ESPI) the light intensity I in the speckle interferogram is given by:

$$I(x,y,t) = I_b(x,y) + I_m(x,y)\cos\left(\Delta\varphi(x,y,t)\right) \tag{1}$$

$I_b = I_R + I_O$ is the background intensity, I_R and I_O are the intensities of the reference wave and the speckled object wave, $I_m = 2\sqrt{I_R\, I_O}$ is the modulation and $\Delta\varphi$ is the phase difference between the reference wave and the object wave to be measured. All these quantities depend on the spatial coordinates (x,y), additionally $\Delta\varphi$ and therefore I too depend on the time t (the minor time dependence of I_O caused by speckle decorrelation is ignored). The aim of ESPI is to measure the temporal course of $I(x,y,t)$ and to calculate from that the course of $\Delta\varphi$ using temporal and spatial phase shifting techniques [1,2].

In praxis these measurements are frequently disturbed by random phase fluctuations. We will confine ourselves to those fluctuations that are caused by pressure and temperature fluctuations in optical fibers, large scale temperature fluctuations in regions where the light is not guided by fibers, mechanical vibrations, and drifts in components. All these effects result in global phase fluctuations $\varphi_g(t)$ that are constant over the field of measurement but vary in time. The phase difference in Eq. (1) is then given by $\Delta\varphi + \varphi_g$.

[1] Address: PF 2503, D-26111 Oldenburg, Germany; E-Mail: heinz.helmers@uni-oldenburg.de; http://aop.physik.uni-oldenburg.de

In [3] we presented a first version of an ESPI-system with integrated active phase stabilization. The system requires no additional optical components and stabilizes the phase $\Delta\varphi + \varphi_g$ at a point P in the field of measurement. Thereby the influence of $\varphi_g(t)$ on the measurement of $\Delta\varphi$ is eliminated. In [4] we reported on the improvement of the phase stabilization scheme by introducing a digital signal processor (DSP) in the system and by increasing its cut-off frequency. In the same paper we introduced first results obtained with an ESPI-system using unresolved speckles. The aim of this paper is to report on further improvements of the digital phase stabilization system and to demonstrate new possibilities which arise from the integration of a CMOS-camera in an ESPI-system using unresolved speckles.

2. IN-LINE DIGITAL PHASE STABILIZATION SCHEME

In the current version of the stabilization system the functionality of further components was integrated into the DSP, thus making the handling of the system and the variation of control parameters even simpler compared to the system described in [4]. The DSP used in the system is a PC-card of type Texas Instrument C67EVM with PCI interface. Once a program is loaded onto the DSP-board via the host PC, it runs on the DSP without charging the host's CPU or bus.

Fig. 1 shows the principal set-up of the system in its current version. The light of a laser diode LD (SDL 5421-G1, 150 mW @ 835 nm) passes through an optical isolator OI (inverse isolation 37 dB) and a half-wave-plate and is coupled into a single-mode polarization maintaining fiber (Scotch 3M HB4611) with a microscopic objective MO. A fiber coupler FC splits the light into an object beam O and a reference beam R. Both beams pass through fibers of about 30 m length, of which some 26 meters are wound on piezoelectric cylinders PZ_R and PZ_O of about 55 mm diameter. The object illuminated by O is imaged by an objective OB with aperture A_{OB} onto the target of either a CCD camera (Sony XC 75 CE, 760×574 pixels) or a CMOS camera (Photonfocus MV-D1024K, 1024×1024 pixels), where its speckled image is superimposed with R, which is directed onto the target by a beam splitter BS. The intensity of R is adjusted by variation of the distance between the end of the fiber and the pinhole PH.

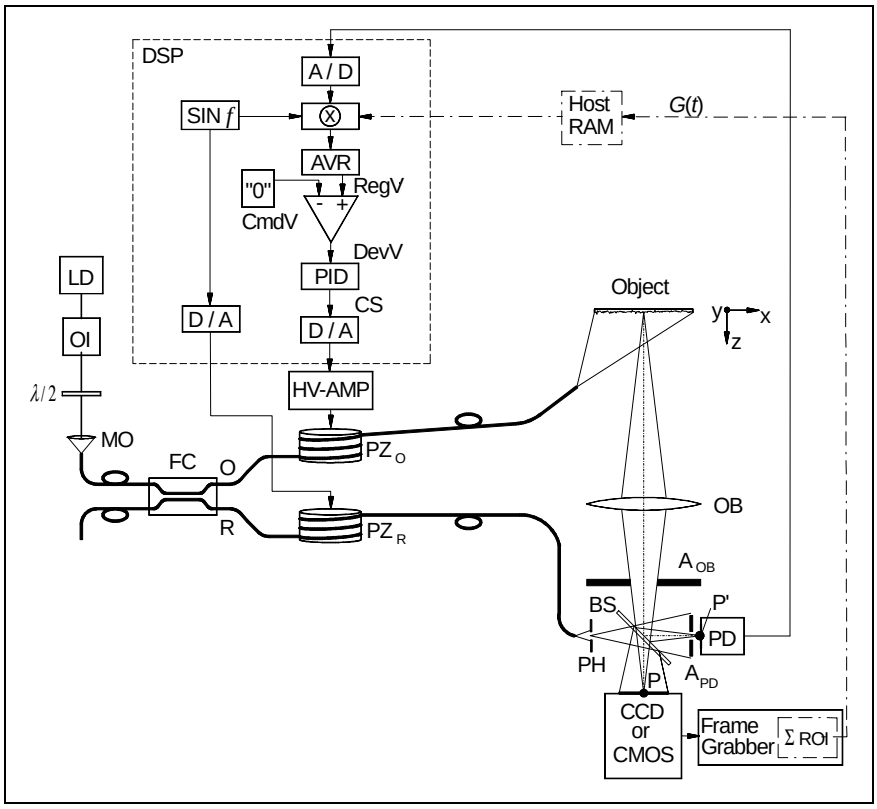

Fig. 1: Set-up of the ESPI-system with integrated active phase stabilization. The connections between the CMOS-camera and the DSP shown by dash-dot lines aren't activated yet.

The phase stabilization is achieved by a synthetic heterodyne technique for which the phase of the reference wave is modulated with frequency f (angular frequency $\omega = 2\pi f$). This is realized by a sinusoidal variation of the optical path of R by changing the diameter of PZ_R with a suitable modulation voltage (SIN f) generated and D/A-converted by the DSP. With α being the amplitude of the phase modulation, the phase difference in Eq. (1) is now given by:

$$\Delta\varphi + \varphi_g + \alpha\sin(\omega t) \coloneqq \Phi + \alpha\sin(\omega t) \tag{2}$$

Inserting Eq. (2) in Eq. (1) and expanding $\cos(\alpha\sin(\omega t))$ and $\sin(\alpha\sin(\omega t))$ in Fourier series gives the intensity I_{PD}, which is measured by the photo detector PD (Hamamatsu photodiode S5973-01 with low noise amplifier) at the point P', where the phase is the same as at the point P:

$$I_{PD} = I_b + I_m \begin{Bmatrix} \cos(\Phi)\left(J_0(\alpha) + 2\sum_{j=1}^{\infty} J_{2j}(\alpha)\cos(2j\omega t)\right) \\ -\sin(\Phi)\left(2\sum_{j=1}^{\infty} J_{2j-1}(\alpha)\sin\left((2j-1)\omega t\right)\right) \end{Bmatrix} \tag{3}$$

with J_j being the Bessel functions of first kind and order j. Eq. (3) shows, that the output signal of PD includes signal components at frequencies $j\omega$. This signal is fed into the DSP and passes in a first step a digital lock-in amplifier. That is, the signal is A/D converted, multiplied with the digital modulation signal, and after that a moving average (AVR) of the product signal is taken over m periods of the modulation signal. The resulting signal (resembling a lock-in output signal) is the regulated value (RegV) of a PID-controller. Finally, the control signal (CS) of the PID-controller is D/A converted and connected to a high voltage amplifier (HV-AMP) which drives the second piezoelectric cylinder PZ_O. PZ_O is the control device in the feedback control system, it can change the phase of the object wave in the range of $\pm 780\ \pi$.

The command value (CmdV) of the PID-controller is set to „0". Therefore, in order to obtain a deviation value (DevV) of „0", the signal RegV has to be „0" too. This is the case, if I_{PD} does not include signal components at the modulation frequency f. Following Eq. (3), this requires $\sin(\Phi) = 0$. Therefore, the PID-controller stabilizes the phase at P' (and P) to a value of $\Phi = 0$ (or integer multiples of π).

A great advantage of the digital control system is the fact, that the parameters f and m together with the corresponding P-, I-, and D-parameters of the control system can be changed very easily and exactly be reproduced. This is particularly important if various variants of the control system shall be worked with (photo detectors with different time constants, change in control devices etc.).

The cut-off frequency of the stabilization system is limited by the modulation frequency f and the number m of periods over which the moving average is taken. f should be set as large as possible and m as small as possible. In the current version we set f = 10 kHz and m = 20. The amplitude α of the phase modulation should be low, so that the modulation in the recorded speckle interferogram is not reduced too much. If the exposure time of the CCD-camera is large compared to $1/f$, the exposure can be calculated from Eq. (1) and (2) and is proportional to the temporal mean of the intensity I_C at the CCD- or CMOS-target:

$$\langle I_C \rangle_t \sim f \int_0^{1/f} I \, \mathrm{d}t = I_b + I_m J_0(\alpha)\cos(\Phi) \tag{4}$$

Thus, the modulation in the recorded speckle interferogram is reduced by a factor $J_0(\alpha)$. At present, we set $\alpha = 30°$ resulting in $J_0(30°) = 0.93$.

Because the amplification-bandwidth product of the photo detector is limited, a low amplification factor A is required if f shall be high. A low value of A can only be achieved if enough light falls onto the detector, which requires enlarging the aperture A_{PD}. The detector then integrates the intensity over n speckles in the speckle interferogram with randomly distributed intensities I and phases φ. Nevertheless, all time dependent phase variations in Eq. (2) still yield a sufficient modulation in the detector signal, as long as these variations are nearly the same for all n speckles within the detectors

aperture A_{PD}. Using results of Lehmann [5] we could show analytically and experimentally [4] that the expected value $<I_m>$ of the modulation in the detector signal increases with $\sqrt{n}$. Therefore, its aperture A_{PD} can be widely opened. Although through this the expected value of the background intensity, $<I_B>$, increases linearly with n, this doesn't affect the detection of the modulation as long as the dynamic range of the detector is high enough. For a photodiode with a dynamic range of 100 dB – 120 dB is this the case.

A further improvement of the system by replacing PD with a small pixel array of a CMOS-camera will be discussed in chap. 4.

3. ANALYSIS OF THE CONTROL SIGNAL

The control signal CS of the phase stabilization system can be used to get additional information about the object movement. If, for example, an object is tilt, phase shifting techniques can only provide the sign of the tilt gradient, but not the sign of absolute displacement. If, on the other hand, the phase is stabilized at the point P (or P'), the sign of the control signal delivers the sign of the absolute displacement, provided the random phase fluctuations φ_g do not overlap the measuring signal to much.

Furthermore, an analysis of the control signal can be used to detect rigid body motions of the object under investigation. This is demonstrated by a simple experiment, where the object was moved forwards and backwards in z-direction by a piezoelectric actuator. The actuator was driven by a sinusoidal sweep signal whose frequency was linearly increased from 0.1 Hz to 10 Hz within 50 s. The amplitude of the object movement was about 0.3 µm. Fig. 2 shows two parts of the temporal course of the corresponding control signal CS(t), from which the periodic rigid body motion can be read easily.

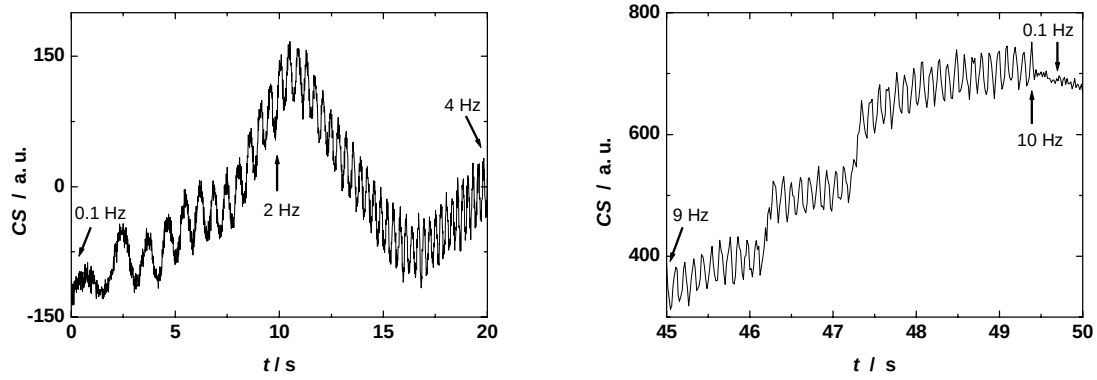

Fig. 2: Two parts of the control signal CS of the stabilization system vs. time t in the case of a periodic rigid body motion of the object with linearly increasing frequency (sweep from 0.1 Hz to 10 Hz within 50 s). The low frequency variations of CS are caused by phase fluctuations in the set-up.

4. REPLACEMENT OF THE PHOTO DETECTOR BY A CMOS-CAMERA

At present, the photo detector PD is used to record the intensity I_{PD} in the interferogram at point P', where I_{PD} is modulated with frequency f. This detector will be obsolete, if a CMOS-camera is used in the set-up instead of a CCD-camera. Such cameras enable a fast readout of small regions of interest (ROI) covering only some pixels of the whole target, e.g. in the vicinity of the point P (see Fig. 1). Adding up the contents (gray values) of the pixels within this ROI yields a resulting gray value G whose temporal course corresponds to that of the signal of PD, provided the readout frequency and the sensitivity of the CMOS-sensor are high enough. Before discussing this aspect in more detail (see chapter 4.2), let us first discuss some general aspects of CMOS-sensors in comparison to CCD-sensors together with some new possibilities in ESPI arising from the use of this type of a sensor.

4.1 CMOS- VS. CCD-SENSORS

Characteristic curve: In CCD-sensors, the interaction of photons with silicon generates photo electrons that are stored in MOS capacitors or in the barrier capacity of photodiodes acting as pixels. The number of electrons, *N*, stored in a pixel is directly proportional to the exposure *E*. During the sequential readout process, the charge within a pixel, $Q = Ne$, (*e* being the elementary charge) is shifted to the readout node (diffusion node) where it is linearly converted to the output voltage. Due to the linearity of the charge accumulation and conversion process the characteristic curve of a CCD-sensor is linear as well as long as the maximum number of electrons that can be stored within a pixel (the full well capacity, fwc) is not exceeded. Otherwise the linear relationship between *E* and *Q* is disturbed and blooming occurs.

In CMOS-sensors, photodiodes act as pixels in which incident photons generate a photocurrent. In integrating sensors (on which we will concentrate ourselves), this current discharges the barrier capacity *C* of the photodiode, which is charged at the beginning of the exposure time. In this case the discharge of *C* by *Q* is proportional to *E*. One important difference between both sensors is the readout process. In CMOS-sensors, the charge to voltage conversion is not done in one common readout node, but in every single pixel, leading there to the voltage $U = Q/C$. As *C* depends on the thickness of the depletion layer of the photodiode which in turn varies with the voltage *U*, the charge to voltage conversion is nonlinear and therefore also the characteristic curve. Fig. 3 shows as an example the characteristic curve of the CMOS-camera Photonfocus MV-D1024K used in our experiments. During the measurement of this curve the camera was operated with those parameters of the so called “LINLOG”-mode, for which the sensor shows the smallest nonlinearity. In a first approximation, the relationship between the exposure and the output gray-value is given by a square-root law. With other parameters, the characteristic curve shows a more logarithmic behavior.

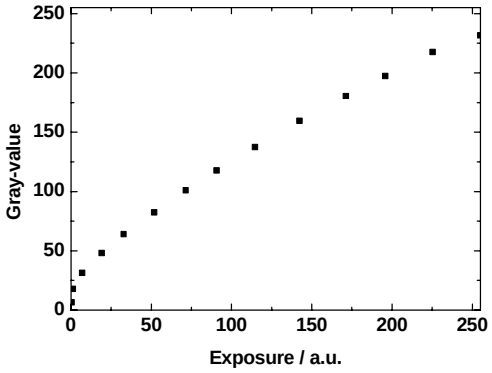

Fig. 3: Characteristic curve of the CMOS-camera Photonfocus MV-D1024K.

At first sight, the nonlinearity of the characteristic curve is only a disadvantage of CMOS-sensors, because the intensity resolution decreases with increasing exposure and the nonlinearity has to be corrected for quantitative interferometry. On the other hand, if the brightness of an object under investigation varies in a large range, the nonlinear characteristic curve may become an advantage. This is demonstrated in Fig. 4, where ESPI deformation fringes on such an object are shown. For the results shown in the left a CCD-camera SONY XC-75 was used. No fringes can be seen in the high reflecting area of the object and blooming occurs (white arrows). In the right, the same situation is shown using the CMOS-camera Photonfocus MV-D1024K. No blooming occurs and deformation fringes are clearly visible on the entire object.

Shutter: In CCD-sensors, the electronic shutter activates all pixels for exposure at the same time by resetting the MOS capacitors or the barrier capacities of the photodiodes. At the end of the exposure time the charge accumulated in the pixels is sequentially transferred to the readout node. In interline transfer sensors, which will be discussed here, the charge is first shifted from the active pixels to their passive neighbors. Because this occurs simultaneously for all pixels, the content of every pixel in the image corresponds to the same instant of the observed scene. The same behavior is obtained by CMOS-sensors using the *global shutter* mode. Here too, every optical sensitive pixel has a passive neighbor where the pixel content can be stored before readout. The shutter in the camera Photonfocus MV-D1024K is of that kind. However, several other CMOS-cameras on the market use *rolling shutters*, where the lines of the sensor are activated and readout sequentially. In this case, different lines in the image represent different instants of the observed

scene, which is useless in most applications. Fig. 5 shows an example of an ESPI deformation measurement using the Vector International CMOS-camera FUGA 15d with 512×512 pixels. Due to the introduced deformation parallel equidistant ESPI-fringes were expected, at left in vertical and at right in horizontal direction, respectively. The deviations from these expectations were caused by temperature fluctuations in the optical fibers (Fig. 1) during the recording of the interferograms.

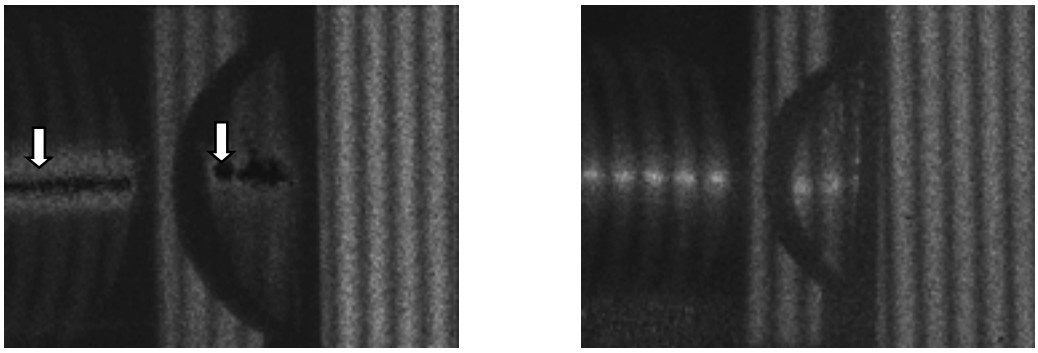

Fig. 4: Results of ESPI-deformation measurements using the set-up of Fig. 7 with unresolved speckles. Left: results obtained using a CCD-sensor with regions of saturation and blooming (white arrows), right: same situation using a CMOS-sensor. (Different image sizes caused by different sensor sizes.)

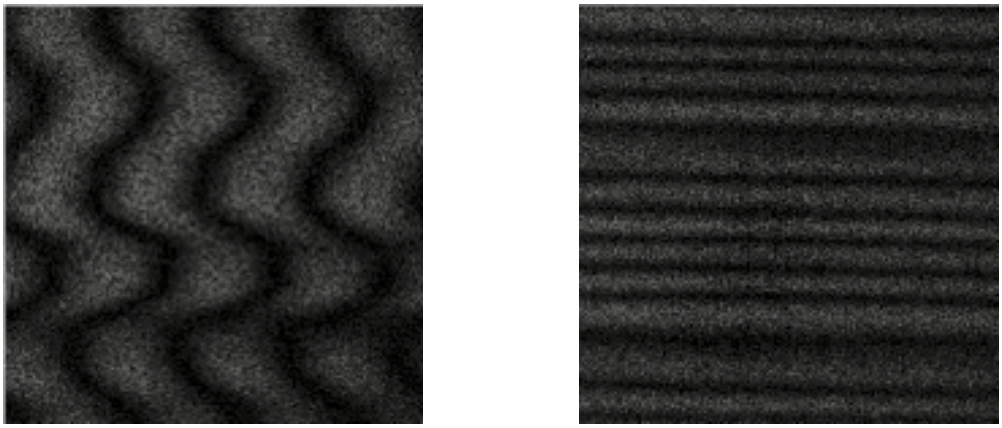

Fig. 5: Results of ESPI-deformation measurements using a CMOS-camera with rolling shutter (FUGA 15d) in the set-up of Fig. 1 with unresolved speckles. Parallel equidistant fringes were expected. Disturbances caused by temperature fluctuations during the readout process.

Regions of interest (ROI): The readout process in a CCD-sensor is based on a sequential charge transfer. Therefore, always the entire sensor has to be readout. This limits the frame rate of high resolution cameras to some 10/s, even if two or four channels are used for readout. In a CMOS-sensor, every pixel can in principle be addressed and readout separately like a memory cell of a RAM. Therefore, regions of interest (ROIs) of the sensor can be readout with high frame rate, which is only limited by the pixel clock of the sensor and the required exposure time. For our camera Photonfocus MV-D1024K, the pixel clock is $f_p = 28$ MHz and the smallest exposure time is $1/f_p \approx 35$ ns. If, for example, an exposure time of 0.5 ms is sufficient and the ROI size is set to 256×256 pixels, a frame rate of about 350/s can be obtained, enabling the observation of fast deformations. Fig. 6 shows an example where a sheet of paper fluttering in the air was used as test object.

Fig. 6: Results of ESPI deformation measurements using the set-up of Fig. 7 with unresolved speckles and a CMOS-camera with a ROI of 512×128 pixels. A sheet of paper fluttering in the air was chosen as object. Exposure time 0.5 ms, time distance between two successive images 4 ms (frame rate 250/s).

4.2 FAST READOUT OF SMALL ROI'S

The photodiode of the photo detector PD which is at present used in the phase stabilization system has an active area of about 0.12 mm^2 and integrates the intensity over some 1000 speckles in order to obtain a sufficient signal amplitude. As mentioned above, it shall be replaced by an adequate ROI of the CMOS-camera within which the content of all pixels will be integrated in order to generate the signal $G(t)$ (see Fig. 1). The pixel pitch of the camera is 10.6 µm. Therefore, an ROI of about 33×33 pixels would be of same size as the aperture of PD. On the other hand, the smallest ROI which can be readout by the camera is of size 128×1 pixels. We therefore started with an ROI of 128×10 pixels, from which only 10×10 pixels are used for signal generation. If an exposure time of 0.5 ms is used, then the maximum frame rate for an ROI of 128×10 pixels is about 1.800/s. Following Nyquists theorem, this means that a modulation frequency of $f \approx 900$ Hz can be used in the stabilization system. As we showed in [3] and [4], this frequency is sufficient in order to get a significant damping of typical phase disturbances in the set-up.

In order to record images with such a high frame rate, to calculate the signal $G(t)$ and to transfer it via the host RAM to the multiplication stage of the DSP (see Fig. 1), special software has to be written. For this purpose we will use functions of Matrox Image Library (MIL) together with special functions of a "Native Library", especially designed for the Matrox Genesis frame grabber used in the set-up. Unfortunately, this software development could not be finished until the manuscript deadline of this paper. Therefore we could only perform some principal tests using the "Image Sequence" option of the Matrox Inspector software, where the maximum frame rate is limited to about 300/s.

For the test we used a simple ESPI set-up with a frequency-doubled Nd:YAG laser of 150 mW optical power at 532 nm. The set-up is shown in Fig. 7; the abbreviations are the same as in the set-up of Fig. 1. The beam ratio was set to $B = \langle I_R \rangle / \langle I_O \rangle \approx 5$. The magnification factor was $M = 0.44$ and the F-number was 3, resulting in a speckle size of 2.84 µm. Because the pixel pitch of the CMOS-camera is 10.6 µm, every pixel is covered by ~ 14 speckles (unresolved speckles). The phase modulation with frequency f was obtained by a mechanical vibration of the object driven by a piezoelectric actuator. The amplitude of the modulation was about 30°, its frequency was $f = 100$ Hz and the exposure time was 0.5 ms. A sequence of 200 images with 128×512 pixels was recorded at a frame rate of about 250/s. From every of these images a ROI of 10×10 pixels covering about 1.400 speckles was selected and the signal $G(t)$ within this ROI was calculated.

Fig. 8 shows the amplitude spectrum of this signal with a significant peak at the modulation frequency of $f = 100$ Hz. That is, the modulation frequency is clearly detectable in the signal of the CMOS-camera, as required for the control system. Taking into account the used exposure time of 0.5 ms, we can furthermore conclude that a modulation signal of about $f = 900$ Hz will be detectable as well, which will be sufficient for a basic version of the stabilization system. Therefore the prerequisites are filled that the detector PD can be replaced by a ROI of the CMOS-camera. This will be verified as soon as the software development mentioned above is completed.

The replacement of PD by a ROI of the CMOS-sensor makes the use of beam splitter BS obsolete. In this case, the fiber end of the reference wave R can be placed in the center of the aperture A_{OB}. By removing BS, the intensity at the camera target is increased by a factor of 2. Therefore, the exposure time can be decreased by the same factor, resulting in a possible frame rate for an ROI of 128×10 pixels of about 3.400/s. Thus, f can be increased to about 1.700 Hz and this will lead to a higher cut-off frequency and therefore to a better performance of the stabilization system.

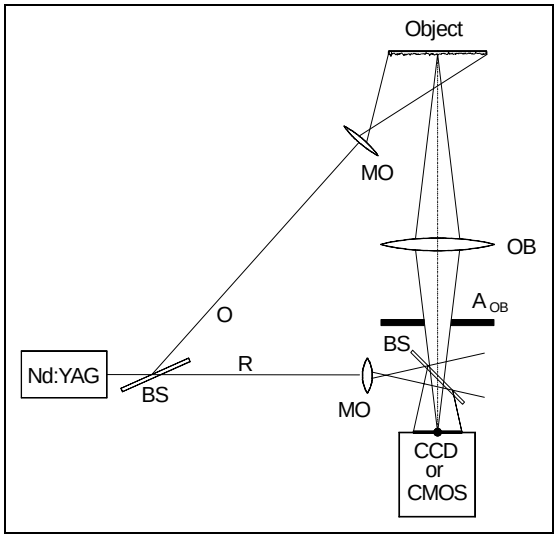

Fig. 7: Simple ESPI set-up to test special capabilities of a CMOS-camera. (Abbreviations see Fig. 1.)

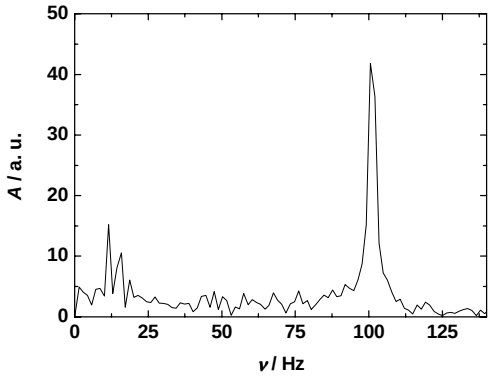

Fig. 8: Amplitude spectrum $A(\nu)$ of the integrated gray value $G(t)$ of a ROI with 10×10 pixels of the CMOS camera. The modulation frequency of the stabilization system at f = 100 Hz is clearly detectable.

5. ESPI-MEASUREMENTS WITH UNRESOLVED SPECKLES AND CMOS-CAMERA

In order to use a ROI of the CMOS-camera instead of the photo detector in the phase stabilization system, the exposure of the target has to be so large that a sufficient amplitude in the signal $G(t)$ is obtained. This requires an opening of the aperture A_{OB} resulting in small speckles. In the set-up shown in Fig. 7 the speckle size was 2.84 µm. Therefore, the speckles are not resolved by the CMOS-sensor but each pixel integrates the intensity over some 14 speckles. In [4] we have shown that the visibility of ESPI deformation fringes is independent from the number n of speckles per pixel, as long as the modulation in the speckle interferograms can be recorded with sufficient resolution, which requires a camera with high dynamic range. This parameter is mainly determined by the full well capacity of the sensor. For the CMOS-camera Photonfocus MV-D1024K used in our experiments the fwc is sufficient (200.000 electrons).

Fig. 9 shows as an example the result of an ESPI deformation measurement using the CMOS-camera Photonfocus MV-D1024K and a beam ratio $B \approx 5$. In the left, correlation fringes are shown that were obtained by simple subtraction of two speckle interferograms representing two different object states. In the right, the pixel contents in the two

interferograms were first corrected in order to compensate the nonlinearity of the characteristic curve of the sensor and after that subtracted. For both cases, the fringe visibility V is nearly the same. In the case of a fringe system with parallel equidistant fringes, V can easily be calculated from the autocorrelation function of the fringe system. For the fringes shown in Fig. 10 we found the same $V = 0.46 \pm 0.01$ with and without compensation of the nonlinear characteristic curve of the sensor. From this we can conclude that for this beam ratio the intensity variations in the interferograms caused by the object deformation are in a range where the characteristic curve of the sensor can be approximated with sufficient accuracy by a linear function.

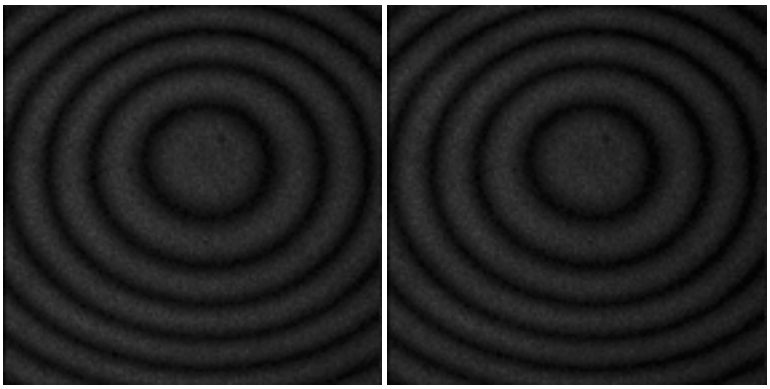

Fig. 9: Results of ESPI deformation measurements using a CMOS-camera in the set-up of Fig. 7 with unresolved speckles. Left without, right with correction of the non-linearity of the characteristic curve.

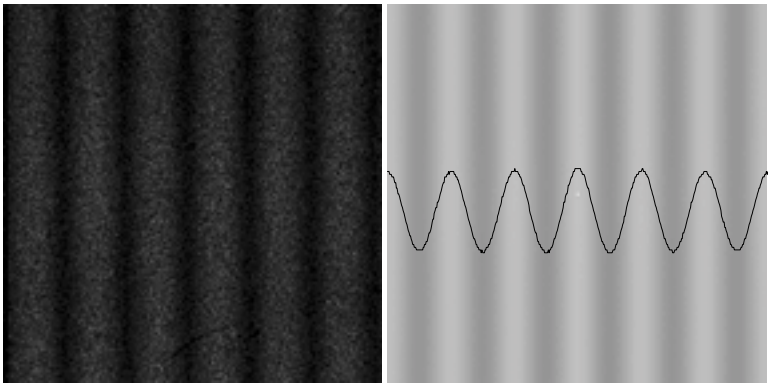

Fig. 10: System of parallel equidistant fringes (left) and modulus of its autocorrelation function with profile scan (right) used to calculate the fringe visibility $V = 0.46 \pm 0.01$.

6. CONCLUSION

We described an ESPI-system with in-line digital phase stabilization where most of the electronic components are integrated in a DSP, making the handling of the system and the variation of parameters of the control system very simple. An analysis of the control signal yielded additional information about the object movement. A high speed CMOS-camera was introduced in the set-up instead of a CCD-camera. It was shown, that this camera can be used for ESPI-deformation measurements with unresolved speckles and that it can simultaneously generate the input signal for the control system. Furthermore it was demonstrated, how specific properties of the camera (high frame rate, nonlinear characteristic curve) can be used for ESPI measurements, where CCD-sensors fail.

REFERENCES

1. Creath, K.: Temporal Phase Measurement Methods, in: Robinson, D. W.; Reid, G. T. [Eds.]: *Interferogram Analysis*, Institute of Physics Publishing, Bristol, 1993, pp. 94-140
2. Burke, J.; Helmers, H.; Kunze, C.; Wilkens, V.: Speckle intensity and phase gradients: influence on fringe quality in spatial phase shifting ESPI-systems, Opt. Commun. 151.1-3 (1998) 144-152
3. Brozeit, A.; Burke, J.; Helmers, H.: Active phase stabilisation in electronic speckle pattern interferometry without additional optical components, Opt. Commun. 173.1-6 (2000) 95-100
4. Helmers, H.; Bischoff, M.; Ehlkes, L.: ESPI-system with active in-line digital phase stabilization, in: Proc. FRINGE '01 (4th Intern. Workshop on Automatic Processing of Fringe Patterns, Bremen, 17. - 19. 9. 2001), 2001, Elsevier, Paris, 673-679
5. Lehmann, M.: Phase-shifting speckle interferometry with unresolved speckles: A theoretical investigation, Opt. Commun. 128 (1996) 325-340